

Nigerian Journal of Physics (NJP)

ISSN online: 3027-0936 ISSN print: 1595-0611

DOI: https://doi.org/10.62292/njp.v34i4.2025.461

Volume 34(4), December 2025



# Assessing the Influence of Aluminum Dopant on the Morphological and Structural Characteristics of NiS Thin Film Material Deposited by Chemical Bath Deposition Technique

\*1Emmanuel Ifeanyi Ugwu, 2Barnaba Abel Adeiza, 3Hilary Uche Igwe and 1Ikpughul Sunday Iyua

<sup>1</sup>Department of Physics, Nigerian Army University Biu, Borno State, Nigeria.

<sup>2</sup>Department of Mechanical Engineering Nigerian Army University, Biu, Borno State, Nigeria.

<sup>3</sup>Department of Industrial Physics, Ebonyi State University Abakaliki, Ebonyi State, Nigeria.

\*Corresponding Author's Email: <u>ugwuei2@gmail.com</u> ORCID iD: <u>https://orcid.org/0000-0001-7045-0814</u>

### **ABSTRACT**

Based on the influence of dopant like aluminum on some sulphide based thin film materials it has become paramount to carry out an assessment of chemical bath deposited Nickel sulphide doped with aluminum has been carried with the intension to ascertain the impact of the dopant concentration on the morphological and structural properties of the as-deposited NiS thin film sample and the aluminum doped, AlNiS thin film with different concentration of aluminum. It was revealed from the result as obtained from the work that both the morphological and structural properties that there were tremendous effect on the crystallinity, grain-size as depicted in figures and computed values in which the values of the lattice constant, dislocation density, micro-strain and grain-size as computed at the same preferred plane within the same diffraction angles are found to vary thereby indicating that there is clear evidence of the effect of aluminum doping concentration on the Nickel sulphide thin film developed with aluminum.

# Keywords:

Assessment,
Aluminum,
Structural and Morphological
properties,
Chemical Bath Deposition,
Dopant,
Nickel sulphide.

#### INTRODUCTION

In the recent years, nanocomposites have been occupying a major focus of research. These nanocomposites are multiphase materials formed by mixing two or more materials. For instance, so many metals especially transition metals (Ti, Sn, Ca, V, Cr, Mn groups) can easily form binary chalcogenide with S, Se, Te etc), and can be synthesized by different methods as such they also exhibit different nanostructures and properties suitable for applications in various fields. Some of them are sulphide, selenide based chalcogenide while some are other are oxide based. Among the various nanocrystalline materials that are chalcogenide based nanocomposites that are often binary in composition are CdS, CdSe, Bi<sub>2</sub>S<sub>3</sub>, PbSe, PbS, As<sub>2</sub>S<sub>3</sub>, Ag<sub>2</sub>S, Cu<sub>2</sub>S, Sb<sub>2</sub>Se<sub>3</sub> ZnS, CaS, PbTe, and NiS while some are ternary CdZnS, CdSSe, CuInSe<sub>2</sub>, PbHgS, CdPbSe, AlNiS etc. (Gupta and Compaan, 2004; Adeyeba et al., 2022; Nefzi et al., 202). Their properties make them beneficial in various applications such as solar energy absorbers, electroconductive coatings, tabular solar collectors, microelectronic devices and gas sensing applications, ion batteries, in superconductors, and heterojunction photodetectors such as Cu2S/CdS,

ZnO/Cu2S,Cu<sub>2</sub>S/ZnS, and Cu2S/n–Si, and sensors (Adelifard *et al.*, 2012; Kassim<sup>a</sup> *et al.*,2011; Guo *et al.*, 2014; Ismail *et al.*, 2020; Zhan *et al.*, 2019; Khan *et al.*, 2018; Soonmin et al., 2022).

However for whichever form appear to be, they can been grown using various deposition techniques the synthetization of sulphide and other chalcogenide based thin films especially NiS and AlNiS thin films viz; vacuum evaporation, photochemical deposition, chemical bath deposition, sputtering, continuous flow microreactor, spray pyrolysis, and successive ionic layer adsorption and reaction technique, (SILAR) (Busar et al., 2020; Kadhim et al., 2017; Leskelä and Ritala, 2003; Kumar and Sankaranarayanan, 2009; Aydin et al., 2014; Owoh and Ugwu, 2009). However, chemical bath deposition technique which is the method we used is one of the most popular techniques for the deposition of thin films due to its advantage over other deposition techniques, such as cost, low pressure, ability to deposit large areas, and low-temperature requirement. It should also be bore in mind that the properties of chemically deposited thin films strongly depend on some deposition parameters, such as deposition time, pH value, bath

temperature, and substrate nature, complexing agent or ligand, doping and annealing (Gashaw and Abza, 2019; Khalil *et al.*, 2019; Ouchtari *et al.*,2011; Ahmed *et al.*, 2021; Okoli *et al.*, 2016 Anuar *et al.*, 2011; Benhaoua *et al.*, 2014; Nefzi *et al.*, 2020; Abdallah *et al.*, 2018; Patel *et al.*, 2016; Obasi *et al.*, 2016).

In general, in whichever form chalcogenide thin films appear to be whether binary or ternary etc they have interesting characteristic associated with many of them. This is a general trend, they are always dark and diamagnetic in nature, insoluble in all solvents, and exhibit semiconducting properties especially n-type semiconductor coupled with the fact that most of them especially NiS have crucial properties, such as nontoxicity, low cost with an ideal energy band gap for so many application (Hedlund *et al.*, 2020; Adeyeba *et al.*, 2022; Kadhim *et al.*, 2017).

Therefore, in this work we intend to assess the effect of variation of aluninium dopping on the morphological and structural properties of NiS as a sulphide based chalcogenide thin film using chemical bath growth technique. That is to ascertain how the variation of concentration of aluminum dopant affects the morphological and structural properties of the thin firm.

# MATERIALS AND METHODS

Prior to the deposition, the glass slide substrates were first of all cleaned by scrubbing thoroughly with cleaned cotton wool and soap solution, rinse with running tap water in order to ensure that all contamination on their surface is removed then further they were ultrasonicate using ultrasonic bath of acetone, methanol and distilled water at room temperature for some hours After that, they were rinsed with deionized water and dried in an open moderate temperature. These cleaning processes were taken in order to ensure complete removal of all the possible impurity (organic or Inorganic) substances from the surface of the substrate which is very important for adherence of the films to the surface of the glass substrate.

The thin films of nickel Sulphide (NiS) were deposited onto the chemically cleaned glass substrates using highly pure chemicals by Chemical Bath Deposition (CBD) process. The chemical bath was prepared by sequential addition of 0.5M of Nickel Chloride Hexa-hydrate (NiCl<sub>2</sub>.6H<sub>2</sub>O), 0.5M of Thiourea, 0.5M of Sodium Hydroxide (NaHO) to neutralize the acidity of the solution, 0.5M of Tri-ethanol-amine (TEA) (C<sub>6</sub>H<sub>15</sub>NO<sub>3</sub>) into three different baths (N, AN<sub>1</sub> and AN<sub>2</sub>. Aluminum Chloride (AlCl) which is the source of Aluminum (Al) served as the doping agent was added into the second and third bath AN<sub>1</sub> and AN<sub>2</sub>) varying from 0.2M to 0.4M. Distilled water was added until the volume of the solution reached 70ml and the PH of the solution was measured using digital PH meter and was kept constant at 8. At a specific temperature, the bath solution was heated and

then thoroughly stirred on a magnetic stirrer for a specific amount of time to aid homogecity. The cleaned and dried substrates were clamped vertically using retort stand, clipped and then lowered into the three beakers (100ml) containing the CBD solution where the Aluminum foil was used as a cover at the top of each beaker in order to prevent dust or unwanted particles from entering the solution. The deposition time was kept constant throughout for each of the samples labelled; N, AN<sub>1</sub> and AN<sub>2</sub>. After that, the three samples were taken out of the bath solution, rinsed in distilled water and dried in an open furnace at moderate temperature at a specific time to remove residual water content and other possible adsorbed surface impurities.

#### **Deduction**

The structural the grain size were deduced from the well-known mathematical as outlined below

The grain-size, of crystallites was calculated using a well know Scherrer's formula

$$D = \frac{0.9\lambda}{\beta\cos\theta} \tag{1}$$

Where D is the grain-size,  $\lambda$  is the wavelength of X-ray used, where ( $\lambda$  = 1.54184Å) gotten from the XRD data,  $\beta$  is the diffraction peak's FWHM and  $\Theta$  is the Bragg's diffraction angle. The estimated grain-size and some other structural data are presented in Table 4.03. This was confirmed that the D values of the films were dependent on the dopant molar concentration

The micro-strain of the films can be calculated using the equation (Busari et al., 2020)

$$\gamma = \frac{\beta}{4\tan\theta} \tag{2}$$

Where  $\epsilon$  is the micro-strain,  $\beta$  is the diffraction peak,  $\Theta$  is the Bragg's angle.

The dislocation density of the films was calculated using the equation below (Adewinbi *et al.*, 2021)

$$\delta = \frac{1}{D^2} \tag{3}$$

Where  $\delta$  is the dislocation density and D is the grain-size as obtained from equation 1, the constants was also determined using the equation below

$$\frac{1}{d^2} = \frac{4}{3} \left[ \frac{h^2 + k}{a^2} \right] + \frac{1}{c^2} \tag{4}$$

Where (d) is the interlunar distance or lattice spacing, (h, k, l) are the miller indices, (a) and (c) are the lattice constants for the film structure. Inter planar spacing can be calculated from Bragg's law as:

$$d = \frac{\lambda}{2\sin\theta} \tag{5}$$

#### **Reaction Equations**

NiCl<sub>2</sub>.  $6H_2O + 2NaOH \rightarrow Ni (OH)_2 + 2NaCl + 6H_2O (8)$   $CH_4N_2S + 2H_2O \rightarrow CO_{2(g)} + 2NH_{3 (g)} H_2S_{(g)} \uparrow \rightarrow S^{2-} + H_2O$ (Undergoing hydrolysis) (6)

Ni (OH)<sub>2</sub> + 2[C<sub>6</sub>H<sub>15</sub>NO<sub>3</sub>]<sub>2</sub> $\rightarrow$  Ni(C<sub>6</sub>HO<sub>15</sub>NO<sub>3</sub>)<sub>2</sub> + 2H<sub>2</sub>O

Ni 
$$(C_6H_{15}NO_3)_2 \rightarrow Ni^{2+} + 2(C_6H_{15}NO_3)$$
 (8)

$$Ni^{2+} + S^{2-} \rightarrow NiS \tag{9}$$

The samples were analyzed using the following techniques such as; X- Ray Diffraction (XRD) and Scanning Electronic Microscopy (SEM) EDX

# RESULTS AND DISCUSSION Energy Dispersive X-ray (EDX) Analysis

The Energy Dispersive X-ray (EDX) analysis (Energy Electron Diffraction Spectrometer) is a technique used for investigating the chemical composition of particles/elements and also the energy decomposition (Kassim *et al.*, 2021). In figure 1a shown below is the

EDX analysis for pure and Aluminum-doped nickel sulphide samples, which shows the sample composed of the nickel with significant amount of Sulphur elements. The EDX result in figure 1a shows the presence of nickel and Sulphur in the pure sample. Also, in figure 1b, the presence of nickel and Sulphur elements are observed together with the presence of Aluminum in the Aluminum-doped samples.

It is observed that both pure and Aluminum-doped samples show the dominance of nickel element which is shown in the figure 2.

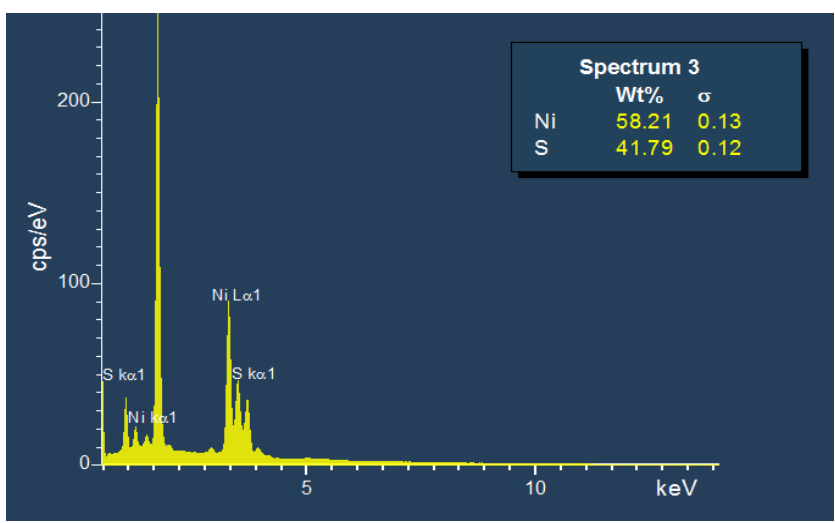


Figure 1(a): EDX image for Pure Sample of Nickel Sulphide

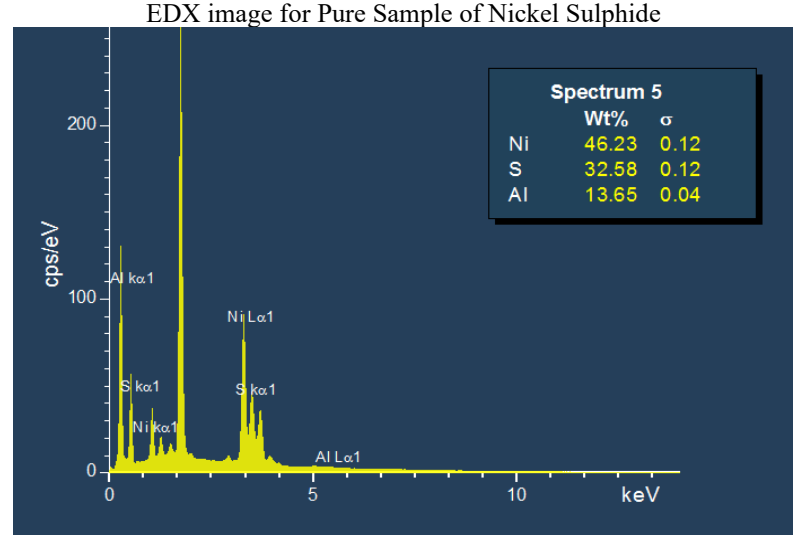


Figure 1(b): EDX image for Aluminum-Doped Sample

# **Surface Morphology**

The scanning electron microscopy (SEM) analysis revealed significant differences in surface morphology between pure nickel sulphide (NiS) films, as shown in the figure 2(a), and those doped with aluminum (Al). The microstructure of undoped NiS film (N) consisted of

unevenly distributed flaky layers with irregular shapes and jagged edges, indicating disrupted growth. Presence of noticeable gaps and porosity between the haphazard clusters evidenced lack of uniformity and discontinuity in the film (Ugwu, 2013; Zhang *et al.*, 2021). Low level Al-doping (AN<sub>1</sub>) led to increased uniformity in layered

structure distribution as flakes appeared smoother with tighter packing, as shown in the figure 2(b), (Chen *et al.*, 2014). Distinct spherical nanocluster formations were observed on the surfaces along with unique cauliflower multivariate shapes implying doping introduced favorable alterations in growth mechanisms as in literature (Patel *et al.*, 2016).

Higher Al-doping  $AN_2$  further enhanced inter-linking between layers, with densely packed smooth textures and negligible porosity between them, as shown in figure 2(c). The surfaces were homogeneously coated with uniformly spread nanoclusters having larger size variants

compared to the low doped films, AN<sub>1</sub> affirming profound impacts of Al-incorporation. The pure NiS, N morphology indicated poor crystalline quality with high structural defects. In contrast, Al doping facilitated reorientation of layered structures leading to significant improvements in density, continuity and nanostructuring. Increased doping concentrations resulted in progressive grain structure modifications, consistent with literature as it affects the doped metal sulphide thin film systems as in (Tejuca *et al.*, 1989) and (Rajathi *et al.*, 2014; Patel *et al.*, 2016).

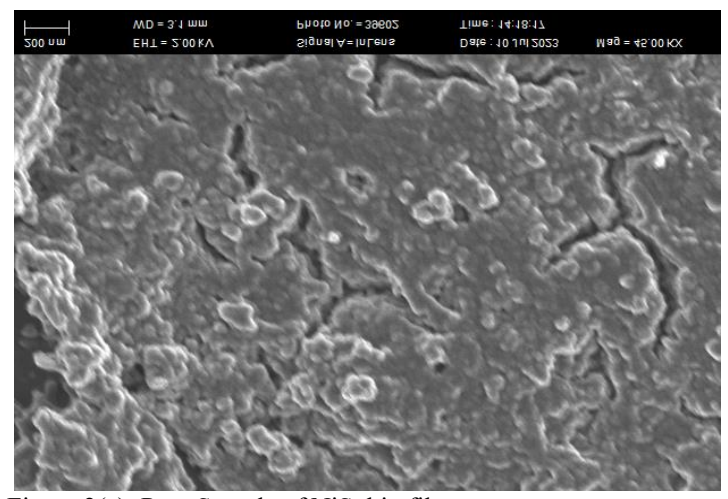


Figure 2(a): Pure Sample of NiS thin film

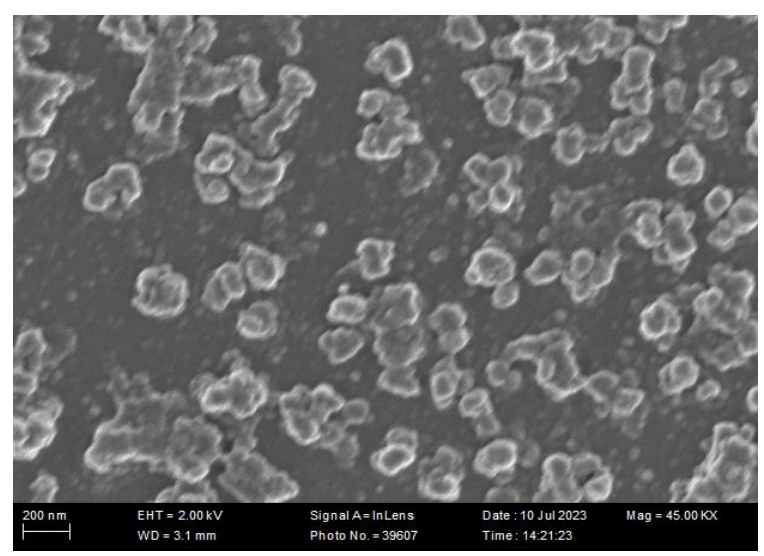


Figure 2(b): Al-doped NiS at 0.2M, N<sub>1</sub>

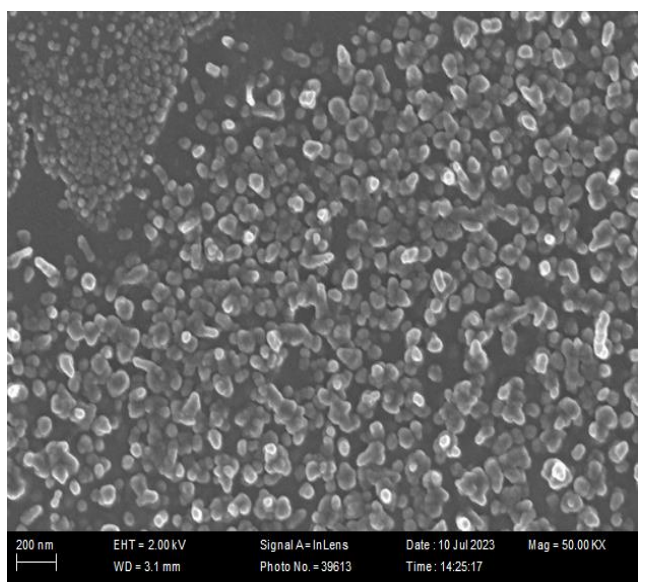


Figure.2(c): Al-doped NiS at 0.4M,N<sub>2</sub>

# Structural X-Ray Diffraction (XRD) Analysis

The structural properties of Nickel sulphide thin film was analyzed using X-Ray Diffraction (XRD) analysis based on the following parameters: crystallinity, grain-size, micro-strain, and dislocation density and lattices parameters. The XRD patterns of the pure Nickel Sulphide thin film N and the Aluminum-doped Nickel sulphide thin films  $AN_1$  and  $AN_2$  at different

concentration of Aluminum doping is shown figure 3. The XRD pattern of Nickel sulphide thin film was taken within the range of Bragg's angle (2 $\Theta$ ), from 10° to 65°. The peaks in the spectra are identified as originating from reflection of (111) and (311) planes indicating the structure of Nickel Sulphide film to be hexagonal in nature. Therefore, having strong orientation in (111) plane.

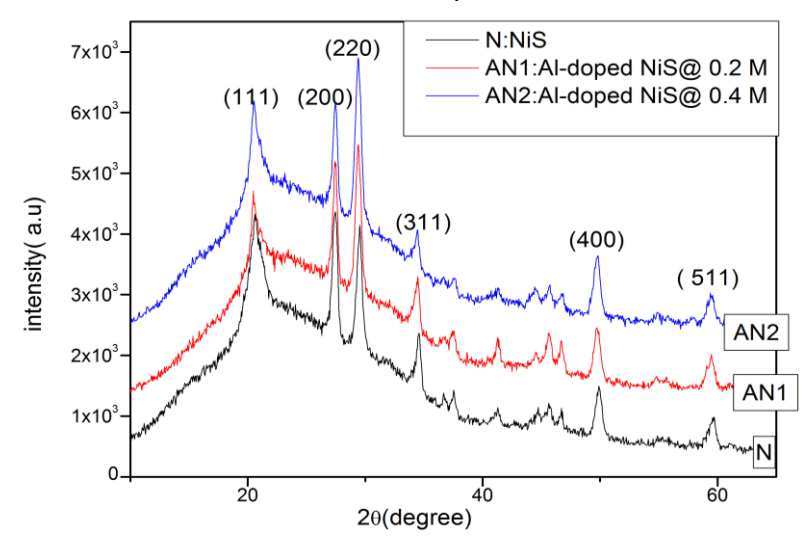


Figure 3: X-Ray Diffraction Pattern of Pure NiS and Al-doped NiS. Thin Films

In a polycrystalline material, the crystallites typically involve differential crystallographic orientation among their neighbors. In relation to some chosen frame of reference, this preference orientation may be dispersed randomly. Here, (311) diffraction plane is the preferred orientation exhibited by the films and similarly, this can be made reference to the XRD pattern of the work done on Cd-O thin film electrodeposited by two electrodes

(Busari *et al.*, 2020). The intensity of the peak is enhanced due to the different concentration in the aluminum-doped nickel sulphide films (i.e., 0.2M and 0.4M).

Where ( $\lambda$ =1.54184) is the wavelength used and  $\theta$  is the incident angle at which maximum diffraction occurs (Patel *et al.*, 2016).

Table 1: Full Width at Half Maximum Angle, Crystallites Size, Micro Strain, Inter Planar Space

S/N	Thin Film/Sample	Bragg's Angle (2Θ)	Preferred Plane (hkl)	d-space(Å)	Grain- size (D) (Å)	Dislocation Density (δ) (Å)	VIICTO-	FWHM (f	Lattice B) constant (a) (Å)	Lattice Constant (c) (Å)
1.	NiS (N)	27.4353	200	3.2666	3.8601	0.0671	0.3957	0.3864	1.7078	1.8229
2.	Al-doped NiS(AN <sub>1</sub> ) @ 0.2M	29.4078	220	3.0375	3.3233	0.0905	0.4295	0.4508	1.6514	1.7716
3.	Al-doped NiS (AN <sub>2</sub> )@ 0.4M	29.4360	220	3.0351	2.4493	0.1667	0.5822	0.6118	1.5923	1.7694

Dislocation Density and Lattice Constant 1 at Preferred Plane (200), (220)

Contrary to expected outcomes, X-ray diffraction studies indicated reduced crystalline domain sizes in aluminumdoped nickel sulfide thin films, concurrently with heightened microstrain and dislocation densities (Shah et al., 2021; Kim et al., 2021). This unintuitive concurrence suggesting aggravated distortion incorporation was further validated through scanning electron microscopy, which evidenced proliferation of granular nanostructures with increasing inter-crystallite voids (Chen et al., 2014). The collective microstructural analyses verify that excessive doping can breach lattice saturation thresholds in nickel sulfide matrices, thereby deteriorating structural arrangements despite additional dopant introduction (Kar et al., 2021). The results emphasize the intricacies of judicious defect engineering by validating aberrant morphologies and porous discontinuities from surpassing optimum incorporation limits that generate accumulated strains without accruing anticipated benefits (Patel et al., 2016). Careful calibrations of dopant quantities within permissible limits are therefore critical for enabling ideal microstructure and performance in synthesized chalcogenide thin films.

#### **CONCLUSION**

Using the chemical bath technique, nickel sulphide thin films were effectively produced in this work at concentrations of aluminum doping whereby it was seen from the EDX result that there was no contamination or impurities in deposited films samples for both asdeposited and aluminum doped NiS thin film. The evaluated and studied of the impact of aluminum doping on the structural and morphological properties of the deposited films obtained from X-Ray Diffraction (XRD) and Scanning Electron Microscopy (SEM) revealed the morphology and the structure characteristics of the deposited films analyzed whereby the outcomes demonstrate that the morphology and structural properties of nickel sulphide thin films are significantly influenced by aluminum dopant. . It was observed that there were slight variations in the structural properties as analyzed here occasioned by different concentration of aluminum doping using XRD analysis. For instance, there is variation in grain-size, grain boundary, dislocation density, micro-grain, lattice parameters and crystalline nature with the aluminum doping concentration as indicated in figures as presented. As from the aspect of the morphology, the SEM micrograph structure revealed that the grain-sizes of the films decrease as the concentration of the aluminum doping increase and this outstanding property of the thin films makes it suitable for various applications and as such can be concluded that the properties of NiS modified by Al dopant have an improved characteristics for optoelectronic, solar harnessing applications as outlined in the literature.

#### REFERENCES

Abdallah B., Ismail A., Kashoua H. and Zetoun, W. (2018). Effects of deposition time on the morphology, structural, and optical properties of PbS thin films prepared by CBD. Journals of nanomaterials.

Adelifard M., Eshghi H. and Mohagheghi M.M.B. (2012). Comparative studies of spray pyrolysis deposited copper sulfide nanostructural thin films on glass and FTO coated glass. Bull. Mater. Sci. 35:739–744.

Adewinbi S. A., Busari R. A., Animasahun L. O., Motoso E. and Taleatu B. A. (2021). "Effective pseadocapacitive performance of binder free transparent  $\alpha$ -U2O3 thin film electrode: Electrochemical and some surface probing", PhydicaB: Condensed Matter 413260. https://doi.org/10.1016/j.physb.2021.413260.

Adeyeba O.A. Ugwu E.I. and Busari R.A. (2022). Influence of Ligand on the Morphological, Electrical, Optical and Solid-State Properties of Chemical Bath Deposited Lead Sulphide Thin Film. Journal of Materials Science Research and Reviews. 10(4):16-31

Ahmed H.S., Mohammed R.Y. and Khalil M.H. (2021,) Effects of Deposition Time and PH on The Characterization of Chemically Synthesized Composite Nano-Wires of Cu2S Thin Films. Sci. J. Univ. Zakho. 9:184–192.

Anuar K, Ho S.M., Lim K.S. and Nagalingam S. (2011). SEM, EDAX and UV-Visible studies on the properties of Cu2S thin films. Chalcogenide Letters. 2011, 8; 405-410.

Aydin E., Sankir M. and Sankir N.D., (2014). Influence of silver incorporation on the structural, optical and electrical properties of spray pyrolyzed indium sulfide thin films. J. Alloy. Compd. 603:119–124.

Benhaoua A., Rahal A. and Benhaoua B. (2014). "Effect of Fluorine doping on the Structural, Optical and Electrical properties of SnO2 thin films prepared spray ultrasonic". Superlattices and Microstructures, 70: 61-69.

Busari M.A., Raheem I. and Sulaiman, K. (2020). Synthesis and Characterization of Ternary and Quaternary Chalcogenide Thin Films. Thin Solid Films, 42(6), 789-802.

Busari R.A., Taleatu B.A., Adewinbi S.A., Adewumi O.E., Omotoso E., Oyedotun K.O and Fasasi, A.Y. (2020). Synthesis and surface characterization of electrodeposited quaternary chalcogenide Cu2ZnxSnyS1+x+2 y thin film as transparent contact electrode, Bull. Mater. Sci. 43:83.

Chen F., Deng D., and Lei Y., (2014). Preparation and photovoltaic properties of the composite based on porous InS films and PCPDTBT. J. Mater. Sci.: Mater. Electron. 25:2244–2247.

Emmanuel Ugwu (2013). Optical and Solid-State Properties of Manganese Sulphide (MnS) Thin Film, Theoretical Analysis, Int. Jnl. of Multiphysics. 11(2): 2017 Zhang X., Du Z. and Li Q. (2021). "Origins of defect generation at high doping levels in sulfide thin films," Journal of Materials Chemistry C, 9:5383-5392

Gashaw H., F. and Abza T. (2019). Short Review of Factors Affecting Chemical Bath Deposition Method for Metal Chalcogenide Thin Films. Int. J. Thin Film. Sci. Technol. 8(3).

Guo K., Chen X., Han J., and Liu Z. (2014). Synthesis of ZnO/Cu2S core/shell nanorods and their enhanced photoelectric performance. J. Sol-Gel Sci. Technol. 72: 92–99.

Gupta A., and Compaan A.D. (2004). All-sputtered 14% CdS/CdTe thin-film solar cell with ZnO: Al transparent conducting oxide. Appl. Phys. Lett. 85:684–686.

Hedlund J.K., Estrada T.G. and Walker A.V. (2020). Chemical Bath Deposition of Copper Sulfide on Functionalized SAMs: An Unusual Selectivity Mechanism. Langmuir. 36:3119–3126.

Ismail R.A., Al-Samarai A.E. and Ali A.M.M. (2020). Effect of molar concentration of CuCl2 on the characteristics of Cu2S film. Opt. Quantum Electron. 52:1–14.

Kadhim A. A., Abdul-Majeed E. I. and Jassim M. M. (2017). "Structural and Optical Properties of PbS Thin Films Deposited by Pulsed Laser Deposited (PLD) Technique at Different Annealing Temperature. International Journal of Physics, 5(1): 1-8. https://www.10.12691/ijp-5-1-1.

Kadhim A., Al-Haddad A. and Abdullah H. (2017). Structural and Optical Properties of NiS Thin Films Grown on Glass Substrates by Pulsed Laser Deposition. Journal of Materials Science and Engineering, 19(3), 789-802

Kar S., Mondal P. and Reddy R. (2021). "Electron microscopy of deteriorated crystallinity in overdoped metal sulfide thin films," iScience, 24:103283.

Kassim A., Ho S. M., Tan W.T. and Ngai C.F. (2011). Influence of Triethanolamine on the Chemical Bath Deposited NiS Thin Films. American Journal of Applied Sciences, 8 (4): 359-361,

Kassim A.N., Min H.S., Siang L.K., and Nagalingam S.A. (2011) SEM, EDAX and UV-Visible studies on the properties of Cu2S thin films. Chalcogenide Lett. 8:405–410

Khalil M.H., Mohammed R.Y. and Ibrahem, M.A. (2021). The Influence of CBD Parameters on the Energy Gap of ZnS Narcissus-Like Nanostructured Thin Films. Coatings. 11:1131.

Khan R., Suhail A. and Sajjad M. (2018). "Sulphide-Based Thin Films for Photovoltaic Applications." Solar Energy Materials and Solar Cells, 187:72-81.

Kim J, Park S, and Han, L., (2021). "Excess doping and materials stability limits in metal sulfide thin films," ACS Applied Nano Materials, 4:7552-7560.

Kumar T. and Sankaranarayanan S. (2009). Growth and characterization of CdZnS thin films by short duration microwave assisted chemical bath deposition technique. Chalcogenide Letters 6(10): 555-562.

Leskelä M. and Ritala M. (2003). Atomic Layer Deposition Chemistry: Recent Developments and Future Challenges. Angew. Chem. Int. Ed. 42:5548-5554.

Nefzi C., Souli M., Cuminal Y. and Kamoun-Turki N. (2020). "Effect of substrate temperature on physical properties of Cu2Fe-SnS4 thin films for photo-catalysis applications". Mater Sci Eng B, Article 114509

Obasi B.I, Osuwa J.C. and Odu D.A. (2016). Effects of varying copper (Cu) ion concentrations of ternary compound of copper iron sulfide (CuFeS) thin films. International Journal of Science and Technology 5(8): 369-373.

Okoli N.L, Udechukwu I.E. and Okpaneje O.T. (2016). Effect of deposition time on optical and solid-state properties of chemically deposited iron copper sulphide (FeCuS) ternary thin films. African Journal of Education, Science and Technology 3(1): 71-8

Ouachtari F., Rmili A., Elidrissi B., Bouaoud A., Erguig H. and Elies P. (2011) Influence of Bath Temperature, Deposition Time and S/Cd Ratio on the Structure, Surface Morphology, Chemical Composition and Optical Properties of CdS Thin Films Elaborated by Chemical Bath Deposition. J. Mod. Phys. 2:1073–1082.

Owoh B. and Ugwu, E.I. (2009). Growth and Optical characterization of Antimony selenide thin film using chemical bath deposition technique. Metallurgy and material engineering, 4(1): 38-41.

Patel R., Shah D. and Desai C. (2016). Influence of Aluminum Doping on the Structural Properties of Nickel Sulphide Thin Films. Thin Solid Films, 72(3): 567-580

Rajathi S., Kirubavathi K. and Selvaraju K. (2014). Structural, Morphological, Optical and Phooluminescence Properties of Nanocrystalline PbS Thin Films Grown by Chemical Bath Deposition. Journal of chemistry.doi: http://dx.doi.org/10.1016/j.arabjc.2014.11.057.

Sagade A. and Sharma R. (2008). Copper sulphide (CuxS) as an ammonia gas sensor working at room temperature. Sensors Actuators B Chem.133:135–143.

Shah D., Patel R. and Q. Chen (2021). "Unexpected defect escalation through doping in nickel sulfide thin films," Acta Materialia, 211:116928.

Soonmin L., Han S. and Kim J. (2022). Chalcogenide Thin Films for Solar Energy Applications. Solar Energy Materials and Solar Cells, 35(4):567-580.

Tejuca L.G., Fierro J.L.G. and Tascon J.M.D. (1989). Advances in Thin Film Deposition Techniques and Their Applications in Sensors, Solar Cells, and Infrared Detectors. Journal of Thin Film Technology 24(2):123-136

Zhan Y., Shao Z., Jiang T., Ye J., Wu X., Zhang B., Ding K., Wu D. and Jie J. (2019). Cation exchange synthesis of two-dimensional vertical Cu2S/CdS heterojunctions for photovoltaic device applications. J. Mater. Chem. A. 8:789–796.